Floquet Phonon Lasing in Multimode Optomechanical Systems

Laura Mercadé,[1,*] Karl Pelka,[2,*] Roel Burgwal,[3,4] André Xuereb,[2] Alejandro Martínez,[1] and Ewold Verhagen[4,3,†]
[1]Nanophotonics Technology Center, Universitat Politècnica de Valencia, Camino de Vera s/n, 46022 Valencia, Spain
[2]Department of Physics, University of Malta, Msida MSD 2080, Malta
[3]Department of Applied Physics and Institute of Photonic Integration, Eindhoven University of Technology, P.O. Box 513, 5600 MB Eindhoven, Netherlands
[4]Center for Nanophotonics, AMOLF, Science Park 104, 1098 XG Amsterdam, Netherlands

(Received 26 January 2021; accepted 15 June 2021; published 10 August 2021)

Dynamical radiation pressure effects in cavity optomechanical systems give rise to self-sustained oscillations or 'phonon lasing' behavior, producing stable oscillators up to GHz frequencies in nanoscale devices. Like in photonic lasers, phonon lasing normally occurs in a single mechanical mode. We show here that mode-locked, multimode phonon lasing can be established in a multimode optomechanical system through Floquet dynamics induced by a temporally modulated laser drive. We demonstrate this concept in a suitably engineered silicon photonic nanocavity coupled to multiple GHz-frequency mechanical modes. We find that the long-term frequency stability is significantly improved in the multimode lasing state as a result of the mode locking. These results provide a path toward highly stable ultracompact oscillators, pulsed phonon lasing, coherent waveform synthesis, and emergent many-mode phenomena in oscillator arrays.

DOI: 10.1103/PhysRevLett.127.073601

Introduction.—Recent times have seen extraordinary progress in exploiting radiation pressure control over optical and mechanical degrees of freedom in optomechanical cavities [1]. The combination of high mechanical coherence and quantum-noise-limited optical control allows the generation of quantum states of macroscopic mechanical resonators [2,3] and quantum transducers [4]. The same advantages enable highly coherent self-oscillations associated with parametric instability [5,6]. Above threshold, a blue-detuned optical drive induces phonon lasing that can be used for timekeeping, microwave oscillators, signal synthesis, and studying nonlinear dynamics [7–11]. The narrow-band high-frequency optical modulation that these oscillations induce connects the microwave and optical domains coherently and offers unchallenged compactness sought after in microwave photonics [12].

If multiple mechanical modes are coupled to a cavity, phonon lasing takes place for the single mode whose threshold condition is satisfied first, whilst other modes get damped [13]. This mechanism of mode competition or gain suppression—which is important to the study of optical lasers as well [14]—generally inhibits multimode phonon lasing using a single optical mode [13]. In optical lasers and parametric oscillators, temporal control techniques such as synchronous pumping [15] circumvent mode competition and establish *mode locking* [16,17] between different lasing frequencies. Two mode-locked tones have equal temporal phase fluctuations [16,17] which has proven extremely powerful in optics; it is the essential mechanism underlying frequency combs leading to spectacular advances in metrology, frequency synthesis, and numerous applications [18]. Simultaneous phononic self-oscillation in multiple modes was reported in low-finesse and strongly pumped narrow-band cavities, but without mode locking [19,20]. A reliable route to mode-locked phonon lasing would enable versatile optomechanical signal synthesis, exploiting coherent wave superposition. It would be especially valuable at high (GHz) frequencies in chip-scale devices for optical or electronic microwave waveform generation and information processing. The mechanism is a defining requirement for studying phonon frequency combs and solitons. Moreover, coherently connecting modes in the blue-detuned pumping regime, characterized by gain and self-oscillation caused by particle-non-conserving interactions, has broad significance in view of the emergent phenomena in non-Hermitian and nonlinear multimode systems, including synchronization [20–28], stability enhancement [29], dynamical topological phases [30], and analog simulators [31].

In this Letter, we overcome the single-mode lasing limitation with a Floquet approach in which the optical drive is modulated in time and show that two mechanical modes are locked via a third Floquet mode similarly to the original mode-locking mechanism outlined in [14]. Recently, time-modulated radiation pressure was used to couple mechanical modes of different frequencies and enable mechanical state transfer [32], nonreciprocity [33], synthetic gauge fields [34], and entanglement [35]. Establishing a Floquet theory for phonon lasing, we show

 © 2021 American Physical Society

that a laser drive modulated at the difference between two mechanical frequencies can induce mode-locked coherent oscillation of both modes. Our general theoretical treatment highlights the capability to establish mode-locked phonon lasing involving multiple modes. We observe the predicted multimode lasing experimentally in a silicon optomechanical crystal cavity supporting two GHz-frequency mechanical modes. The long-term stability of the output microwave tones is significantly improved, promising application for highly stable, ultracompact oscillators in microwave photonics.

Theoretical model.—We consider the collective dynamics of a system consisting of N mechanical modes (labeled by j) coupled to one optical mode, described by the Hamiltonian

$$\hat{H}_S/\hbar = \omega_{\mathrm{op}}\hat{a}^\dagger\hat{a} + \sum_{j=1}^{N}[\Omega_j\hat{b}_j^\dagger\hat{b}_j - g_j\hat{a}^\dagger\hat{a}(\hat{b}_j + \hat{b}_j^\dagger)], \tag{1}$$

with $\hat{a}$ ($\hat{b}_j$) referring to the optical (mechanical) annihilation operator, ω_{op} (Ω_j) referring to the corresponding resonance frequencies, and g_j referring to the vacuum optomechanical coupling rates. The driving laser is modeled by adding $i\hbar[\mathcal{E}_{\mathrm{drive}}(t)\hat{a}^\dagger - \mathcal{E}^*_{\mathrm{drive}}(t)\hat{a}]$ to the Hamiltonian, assuming $\mathcal{E}_{\mathrm{drive}}(t) = \mathcal{E}_0 e^{i\omega_L t}\mathcal{T}(t)$ with $\mathcal{T}(t)$ implementing optical modulation. Appending bath degrees of freedom and tracing them out [1] yield quantum Langevin equations. These are separable into mean field and fluctuation components [$\hat{a}(t)e^{i\omega_L t + i\phi_0} = \alpha(t) + \hat{\mathfrak{a}}(t)$ and $\hat{b}_j(t) = \beta_j(t) + \hat{\mathfrak{b}}_j(t)$], with linearized fluctuation dynamics

$$\dot{\hat{\mathfrak{a}}} = -\left(i\Delta + \frac{\kappa}{2}\right)\hat{\mathfrak{a}} + i\sum_{j=1}^{N} g_j[\alpha\Re(\hat{\mathfrak{b}}_j) + \hat{\mathfrak{a}}R(\beta_j)] + \sqrt{\kappa}\hat{\mathfrak{a}}_{\mathrm{in}},$$
$$\dot{\hat{\mathfrak{b}}}_j = -\left(i\Omega_j + \frac{\Gamma_j}{2}\right)\hat{\mathfrak{b}}_j + ig_j(\alpha^*\hat{\mathfrak{a}} + \alpha\hat{\mathfrak{a}}^\dagger) + \sqrt{\Gamma_j}\hat{\mathfrak{b}}_{j,\mathrm{in}}. \tag{2}$$

Here, the optical field is considered in a frame rotating at the central laser frequency ω_L and $\Delta = \omega_{\mathrm{op}} - \omega_L$ denotes the laser detuning. We introduced the optical (mechanical) decay rate κ (Γ_j), input noise operators $\hat{\mathfrak{a}}_{\mathrm{in}}$ ($\hat{\mathfrak{b}}_{j,\mathrm{in}}$), $\Re(\hat{o}) = \hat{o} + \hat{o}^\dagger$, and $R(z) = z + z^*$. For periodic modulation $\mathcal{T}(t) = \sum_m \mathcal{T}_m e^{-im\Omega_{\mathrm{mod}}t}$ ($m \in \mathbb{Z}$), the mean optical field α inherits the periodicity and admits a Floquet ansatz. We implement laser intensity modulation by $\mathcal{T}_0 = [1 - i\mathcal{J}_0(d)]/2$, $\mathcal{T}_{\pm 1} = -\mathcal{J}_1(d)/2$, where $\mathcal{J}_m$ denotes the mth Bessel function of the first kind and d the modulation depth, to find $\alpha(t) = \sum_n \bar{\alpha}_n e^{-in\Omega_{\mathrm{mod}}t}$ where the coefficients $\bar{\alpha}_n$ have to be deduced numerically if $\mathcal{T}_{\pm 1} \neq 0$ (see Supplemental Material [36], which includes [37], for more details). The dynamics of fluctuation components $\hat{\mathfrak{a}}$ and $\hat{\mathfrak{b}}$ turn into a periodic system that can be treated with Floquet techniques [38,39]:

$$\dot{\hat{\mathfrak{a}}}^{(0)} = \tilde{\chi}^{-1}\hat{\mathfrak{a}}^{(0)} + \sum_n\sum_{j=1}^{N} ig_j\bar{\alpha}_n\Re(\hat{\mathfrak{b}}_j^{(n)}) + \sqrt{\kappa}\hat{\mathfrak{a}}_{\mathrm{in}}^{(0)},$$
$$\dot{\hat{\mathfrak{b}}}_j^{(n)} = \check{\chi}_{jn}^{-1}\hat{\mathfrak{b}}_j^{(n)} + ig_j[\bar{\alpha}^*_{-n}\hat{\mathfrak{a}}^{(0)} + \bar{\alpha}_n\hat{\mathfrak{a}}^{\dagger(0)}] + \sqrt{\Gamma_j}\hat{\mathfrak{b}}_{j,\mathrm{in}}^{(n)}, \tag{3}$$

with the mechanical Floquet susceptibilities $\check{\chi}_{jn}^{-1} = -[i(\Omega_j - n\Omega_{\mathrm{mod}}) + \Gamma_j/2]$ and the optical susceptibility $\tilde{\chi}^{-1} = -\{i[\Delta - \sum_j g_j|\bar{\alpha}_0|^2 I(\check{\chi}_{j0}^{-1})/|\check{\chi}_{j0}^{-1}|^2] + \kappa/2\}$ where we denote $I(z) = i(z^* - z)$. Using the input-output relations for the relevant contributions to the optical field $\hat{\mathfrak{a}}_{\mathrm{out}}(\omega) = \hat{\mathfrak{a}}_{\mathrm{in}}^{(0)}(\omega) - \sqrt{\kappa}\hat{\mathfrak{a}}^{(0)}(\omega)$ with input noise obeying $\langle\hat{\mathfrak{u}}_{\mathrm{in}}^{(m)}(\omega)\hat{\mathfrak{w}}_{\mathrm{in}}^{\dagger(p)}(\omega')\rangle = \delta(\omega-\omega')\delta_{\mathfrak{u}\mathfrak{w}}\delta_{mp}(\mathfrak{n}_{\mathrm{th}}^{\mathfrak{u}} + 1)$ yields the stationary power spectral density of the experimentally accessible output field

$$S(\omega) = \tilde{S} + \sum_{n,j}\frac{\kappa g_j^2|\bar{\alpha}_n|^2\Gamma_j\bar{n}_j}{[(\omega - \bar{\Delta})^2 + \frac{\kappa}{4}][(\omega - \Omega_{jn})^2 + \frac{\Gamma_j^2}{4}]}, \tag{4}$$

consisting of a noise floor $\tilde{S}$ and multiple Lorentzian peaks at $\Omega_{jn} = \Omega_j + n\Omega_{\mathrm{mod}}$, filtered by the cavity density of states. This is of Lorentzian form, with effective detuning $\bar{\Delta} = \Delta + \sum_{j,n} 2g_j^2|\bar{\alpha}_n|^2/\Omega_j$, due to static radiation pressure for $\Gamma_j \ll \Omega_j$.

Stability analysis.—To evaluate the mechanical stability, we eliminate the optical fluctuation operator $\hat{\mathfrak{a}}^{(0)}$ in Eq. (3) and analyze its effect on the Floquet modes of the mechanical degrees of freedom which are coupled via

$$\sigma_{jlp}^{(m)}(\omega) = \frac{g_j g_l\bar{\alpha}^*_{-m}\bar{\alpha}_p}{i(\bar{\Delta} - \omega) + \frac{\kappa}{2}} - \frac{g_j g_l\bar{\alpha}_m\bar{\alpha}_p^*}{-i(\bar{\Delta} + \omega) + \frac{\kappa}{2}}. \tag{5}$$

The stationary mechanical spectra without periodic drive ($m \equiv p \equiv 0$) are the well-known Lorentzians [40,41] $S_{\hat{\mathfrak{b}}_j}(\omega) = \tilde{S}_{\hat{\mathfrak{b}}_j} + \Gamma_j\bar{n}_j[(\Omega_j' - \omega)^2 + \Gamma_j'^2/4]^{-1}$ with optical-spring-corrected frequencies $\Omega_j' = \Omega_j\sqrt{\mathrm{I}[\sigma_{jj0}^{(0)}(\Omega_j)]/4 + 1}$ and modified linewidths $\Gamma_j' = \Gamma_j + R[\sigma_{jj0}^{(0)}(\Omega_j)]$.

The latter allow one to assess the mechanical oscillators' stability for blue-detuned driving ($\bar{\Delta} < 0$): their decay rates Γ_j' are composed of intrinsic dissipation Γ_j counteracted by the stimulated emission process $\sigma_{jj0}^{(0)}(\Omega_j)$ (see Supplemental Material [36]). In this stimulated process for $\hat{b}_j$, a cavity photon with excess energy of (approximately) $\hbar\Omega_j$ and a stimulating phonon are converted into a (approximately) resonant photon and two coherent phonons of this mode. Its rate overcoming the decay rate Γ_j indicates surpassing the threshold of self-sustained oscillation ($\Gamma_j' < 0$).

In the presence of the periodic drive, additional processes associated with $\sigma_{jl\pm1}^{(0)}\sigma_{jl0}^{(\pm1)}(\Omega_j)$ for $l \neq j$ modify the decay rates

$$\Gamma_j'' = \Gamma_j' - \sum_{l\neq j} R\left[\frac{\sigma_{jl\pm1}^{(0)}\sigma_{jl0}^{(\pm1)}}{i(\Omega_l - \Omega_j \mp \Omega_{\mathrm{mod}}) + \frac{\Gamma_l}{2} + \sigma_{jl\pm1}^{(\pm1)}}\right], \quad (6)$$

which can become prominent if in addition to the detuning being resonant the modulation frequency is tuned into resonance at (approximately, on the scale of the mechanical linewidth) the difference of distinct mechanical frequencies $\Omega_{\mathrm{mod}} = |\Omega_j - \Omega_l|$ for low modulation depths $[I(\sigma_{jl\pm1}^{(\pm1)}) \ll |\Omega_j - \Omega_l|]$. These additional contributions can be interpreted as the stimulated emission of a cavity photon and a phonon creating a coherent phonon in a different mode (see Supplemental Material [36]). This process can act as a seed of mode locking between the two mechanical modes and cause a mode that exceeds the threshold ($\Gamma_j'' < 0$) to stimulate simultaneous lasing of the other mode, circumventing the prohibitive effect of gain saturation.

To verify the existence of a multimode phonon lasing state, we conduct numerical simulations of the Itô stochastic differential equation for the mean field dynamics employing the Euler–Maruyama scheme [42] (see Supplemental Material [36]) as depicted in Fig. 1. We choose an instructive set of parameters for two mechanical modes ($N = 2$, $\Omega_1 = 5.3$, $\Gamma_1/\Omega_1 = 0.16$, $g_1 = 0.80$, $\Omega_2 = 7.1$, $\Gamma_2/\Omega_2 = 0.10$, $g_2 = 1.1$) and the optical cavity ($\Delta = -6.1$, $\kappa = 3$). Driving this system with $\mathcal{E}_0 = 8.9$, leading to $\bar{\Delta} \approx -\Omega_1$, while modulating with depth $d = 0.08$ for various modulation frequencies Ω_{mod} reveals the effect of intensity modulation when starting from a thermal state. Figure 1(b) shows that for off-resonant modulation ($\Omega_{\mathrm{mod}} \ll \Omega_2 - \Omega_1$) the mechanical modes stay in a thermal state, as the system is just below the instability threshold for the chosen power. For modulation closer to resonance, only one of the modes (β_1) transitions from thermal into self-sustained oscillations, with a high amplitude and narrow spectrum as expected for a lasing process [Fig. 1(c)]. This happens because of the additional negative damping contribution in Eq. (6). That extra modulation-induced process involves the other mechanical mode (β_2), as evidenced by the fact that β_2 is coherently driven at frequencies $\tilde{\Omega}_1$ and $\tilde{\Omega}_1 + \Omega_{\mathrm{mod}}$, while it still does not show significant narrowing [magenta spectrum in Fig. 1(c)]. This lack of narrowing of the linewidth signifies that β_2 is not lasing for this particular off-resonant driving. This changes when the modulation frequency is tuned into resonance at approximately the difference of the mechanical frequencies [Fig. 1(d)], and the multimode process gain, described by Eq. (6), is maximized. Then, both mechanical modes undergo coherent oscillation at distinct frequencies resulting in multimode oscillation (MMO) since *both* peaks in the mechanical spectra are described by Lorentzians with decreased linewidth and not by the sum of the thermal Lorentzian and additional peaks, as in Fig. 1(c).

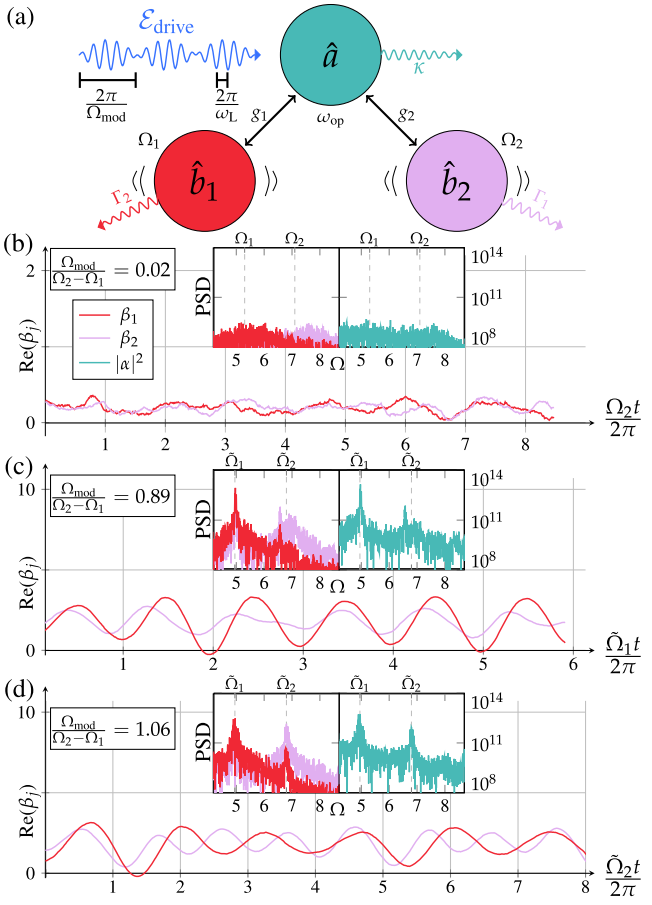

FIG. 1. (Color online) Multimode phonon lasing in an optomechanical cavity. (a) Two mechanical modes at distinct frequencies are coupled to an optical cavity driven by an intensity-modulated pump. (b) For small modulation frequency both mechanical modes remain in a thermal state. (c) With the modulation frequency approaching the difference frequency only one mode (β_1) transitions into SSO with the help of the multimode gain mechanism, whereas the other mode remains in the thermal state while being driven at $\tilde{\Omega}_1 + \Omega_{\mathrm{mod}}$. (d) When the modulation frequency approximates the difference frequency, both mechanical modes coherently oscillate, i.e., MMO occurs. Insets show the power spectral densities of the mechanical (left) and optical (right) modes.

Experimental multimode phonon lasing.—To confirm the predicted MMO state experimentally, we use the 1D silicon optomechanical crystal cavity depicted in Fig. 2(a). It supports a high-quality optical mode [Fig. 2(b)] that allows phonon lasing under blue-detuned laser driving [10]. Interestingly, this system hosts two GHz-frequency mechanical modes within the beam's phononic bandgap labeled 'P1' and 'P2,' corresponding to oscillations of the lateral corrugations [43]. Their displacement is depicted in Fig. 2(c), simulated using the shape retrieved from electron microscopy. Figure 2(d) shows both modes' thermomechanical spectra transduced at low power. All measurements were performed at room temperature and

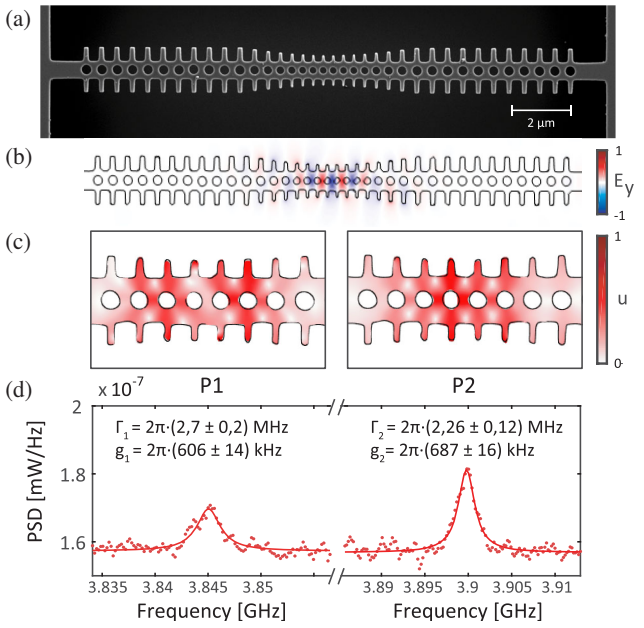

FIG. 2. (a) Scanning electron microscope image of the fabricated optomechanical cavity. (b) Simulated electric field pattern of the optical mode. The measured resonance wavelength is $\lambda_r = (1527.4 \pm 0.2)$ nm with loaded decay rate $\kappa/2\pi = (14.88 \pm 0.08)$ GHz. (c) Calculated mechanical displacement profiles of P1 and P2. (d) Measured power spectral density of the thermally transduced mechanical modes at $\Omega_1/2\pi = 3.845$ GHz and $\Omega_2/2\pi = 3.899$ GHz.

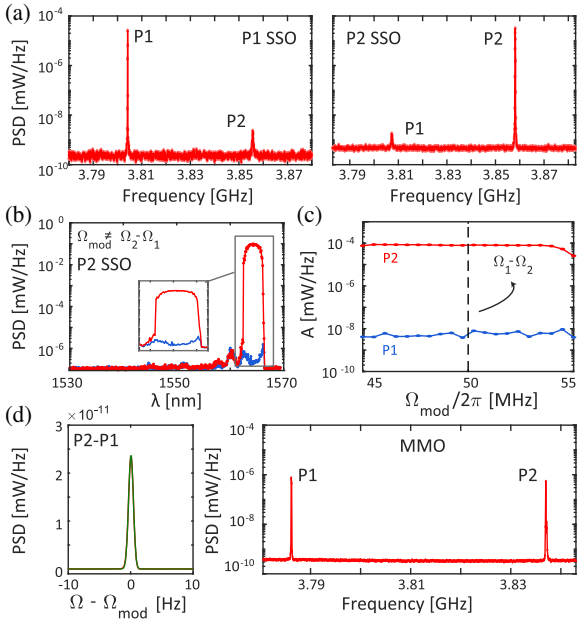

FIG. 3. From single-mode to multimode phonon lasing. (a) Self-oscillation spectra of P1 (left) and P2 (right), without external modulation. (b) P2 SSO excitation through a wavelength scan with a blue-detuned laser $\Omega_{\rm mod} \neq \Omega_2 - \Omega_1$. (c) Mechanical amplitude evolution in a modulation frequency scan around the difference frequency when P2 is self-oscillating showing that hysteretic effects prohibit the MMO state from being activated from the SSO state. (d) Multimode lasing under an input modulation $\Omega_{\rm mod} = \Omega_2 - \Omega_1$. Left: difference tone obtained by mixing the lasing mechanical modes in the microwave domain, proving mode locking. Right: spectrum of the two mechanical modes when lasing simultaneously (MMO state).

atmospheric pressure, coupling light to and from the cavity with a dimpled fiber taper (see more details in the Supplemental Material [36]). Notably, the coupling rate and damping of both mechanical modes are quite similar, yielding similar cooperativities $C_j = 4g_j^2\bar{n}_c/(\Gamma_j\kappa)$, with $\bar{n}_c$ the intracavity photon number: $C_1/\bar{n}_c = (3.7 \pm 0.3) \times 10^{-5}$ and $C_2/\bar{n}_c = (5.6 \pm 0.4) \times 10^{-5}$.

Because of this similarity, we observe that either mode can be individually driven to a single-mode self-sustained oscillation (SSO) state under blue-detuned driving, as shown in Fig. 3(a). The choice of lasing state depends on fine experimental conditions, including the initial (random) thermal state of each mode. Figure 3(b) depicts both modes' intensities while the laser wavelength (input power $P_{\rm in} = 3.16$ mW) is continuously increased toward the SSO regime. We see that once one mechanical mode (P2) starts lasing, the other mechanical mode (P1) is damped, evidencing gain suppression [13]. We then modulate the laser intensity at frequency $\Omega_{\rm mod}$ (with $d = 0.18$). Starting from P2 in an SSO state and stepping the modulation frequency across resonance $\Omega_{\rm mod} = \Omega_2 - \Omega_1$ does not activate the MMO state, as the thermomechanical Lorentzian of P1 remains unaffected due to gain suppression [see Fig. 3(c) and Supplemental Material [36]]. Instead, the MMO regime is reached when the intermodal coupling is established already before the threshold is reached, allowing the Floquet modes to cross the threshold simultaneously, indicating hysteretic behavior (see Supplemental Material [36]). We experimentally achieve this by implementing the modulation fixed to the measured difference frequency, and then tuning a far-blue-detuned laser toward cavity resonance. The resulting MMO state is shown in Fig. 3(d) (right): both modes are simultaneously in the self-sustained regime at very different frequencies. The left panel shows the beat note of the two lasing tones, measured after mixing them and filtering out the modulation at $\Omega_{\rm mod}$ (see Supplemental Material [36]). Its extremely narrow linewidth, much smaller than the linewidths of the individual tones and only limited by the 1 Hz resolution bandwidth of the spectrum analyzer, proves the mode locking of the two lasing phonon modes: the beat note phase evolves as the difference of the oscillator phases $\tilde{\Omega}_j + \phi_j(t)$, with all fluctuations contained in $\phi_j(t)$. Its narrow spectrum proves $\phi_2(t) - \phi_1(t)$ is constant, i.e., the modes' phase fluctuations are identical—they are mode locked. We emphasize that without the modulated drive, the modes cannot self-oscillate independently as required in synchronization [44].

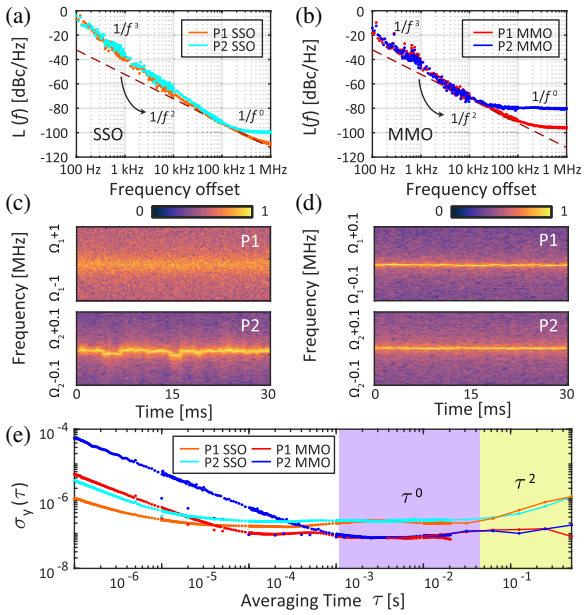

FIG. 4. Phase noise and stability behavior. Phase noise of P1 (blue) and P2 (red) in the SSO (a) and MMO regimes (b). Time evolution of the recorded spectra for the P1 (top) and P2 (bottom) modes for SSO lasing in mode P2 (c), and for MMO lasing (d). (e) Allan deviation for P1 and P2 in the SSO and MMO states.

Phase noise and stability analysis.—To characterize the linewidth and stability of the oscillators, we analyze their phase noise $L(f)$ in the SSO and MMO states in Figs. 4(a) and 4(b). In both cases we observe the typical noise contributions expected in optomechanical oscillators, i.e., white phase ($1/f^0$), white frequency (random phase walk, $1/f^2$), and flicker frequency ($1/f^3$) noise [10], in good agreement with Leeson's model [45]. A phase noise of (-65 ± 3) dBc/Hz at 10 kHz is measured for the SSO state, on par with other optomechanical microwave oscillators [10,11,46–48]. Although white phase and flicker frequency noise are dominating, we estimate a Lorentzian linewidth of maximally ~40 Hz from the fitted contribution of the random phase walk.

Interestingly, the phase noise of the MMO state is (-70 ± 4) dBc/Hz at 10 kHz; thus, it is smaller than that in the SSO regime for this and all smaller offset frequencies. This reduction of fluctuations is also clear from the time evolution of the spectra in the SSO (P2) and MMO states, presented in Figs. 4(c) and 4(d). All traces presented here correspond to mechanical modes in the lasing state, excluding the thermally driven P1 mode [top panel of Fig. 4(c)], which requires a different frequency span. The observed jitter of the lasing frequency of P2 in Fig. 4(c) could stem from thermal, optical power, and fiber taper fluctuations influencing the optical spring effect, as Eq. (5) implies. In the MMO lasing state [Fig. 4(d)], we observe a significantly enhanced stability of both lasing modes.

Figure 4(e) shows the Allan deviation $\sigma_y(\tau)$ [49], obtained from combining the phase noise measurements in Figs. 4(a) and 4(b) and the spectral time traces for longer acquisition times (up to 1 s). For low averaging times τ the main differences between the Allan deviations stem from the white phase noise background, which is related to measurement sensitivity and signal amplitude. However, for longer averaging times [purple shaded area in the middle of Fig. 4(e)], where the dominant source of fluctuations is flicker frequency noise (τ^0), the MMO is significantly more stable than the SSO state. This is in agreement with the obtained root-mean-square jitter, which reduces from 220 ± 5 ps in both SSO states to 76 ± 5 ps in the MMO state (see Supplemental Material [36], which includes Ref. [50], for more details). Also for high averaging times with a frequency drift contribution [τ^2, yellow shaded area in the right part of Fig. 4(e)], the multimode stability is superior. This improvement cannot be ascribed to locking to the external modulation, as that is far off resonant. Instead, it could be related to the MMO regime being sustained at significantly reduced intracavity power, as suggested by the relative heights in Fig. 3, thus reducing the influence of optical fluctuations on the optomechanical spring effect [51]. Here, the effective mass is increased in the system once both mechanical modes are in the lasing state, a feature that also occurs in synchronized oscillators [29,52]. This effect could very well be in play here, with an associated 3 dB reduction of phase noise expected when the two oscillators are coupled. Future studies should reveal the various contributions and the application potential of the increased stability in the Floquet lasing regime.

Conclusion.—Our investigation shows that nonlinear dynamics of Floquet modes enable mode-locked multimode phonon lasing in optomechanical systems. It can be understood from higher-order cross-mode corrections to the self-energy for modulated drive. We demonstrated this prediction experimentally, revealing that it enhances long-term oscillator stability. The demonstrated mechanism generalizes to systems with many equally spaced (GHz) modes [53] where it could be employed toward phononic frequency combs, and can be used to study the rich emergent physics of many-mode self-oscillating optomechanical systems, in a fully controllable fashion.

The authors thank Javier del Pino for useful discussions. This work is supported by the European Union's Horizon 2020 research and innovation program under Grant Agreements No. 732894 (FET Proactive HOT), 713450 (FET-Open PHENOMEN), and 945915 (SIOMO), the Spanish State Research Agency (PGC2018-094490-B-C21) and by the Juilan Schwinger Foundation project grant No. JSF-16-03-0000 (TOM). It is part of the research program of the Netherlands Organisation for Scientific Research (NWO). A. M. acknowledges funding from Generalitat Valenciana under Grants No. PROMETEO/

2019/123, BEST/2020/178, and IDIFEDER/2018/033. E. V. acknowledges support from the European Research Council (ERC Starting Grant No. 759644-TOPP).

*These authors contributed equally to this work.
†verhagen@amolf.nl

[1] M. Aspelmeyer, T. J. Kippenberg, and F. Marquardt, Rev. Mod. Phys. **86**, 1391 (2014).
[2] J. Chan, T. P. M. Alegre, A. H. Safavi-Naeini, J. T. Hill, A. Krause, S. Gröblacher, M. Aspelmeyer, and O. Painter, Nature (London) **478**, 89 (2011).
[3] J. D. Teufel, T. Donner, D. Li, J. W. Harlow, M. S. Allman, K. Cicak, A. J. Sirois, J. D. Whittaker, K. W. Lehnert, and R. W. Simmonds, Nature (London) **475**, 359 (2011).
[4] C. A. Regal and K. W. Lehnert, J. Phys. Conf. Ser. **264**, 012025 (2011).
[5] T. J. Kippenberg, H. Rokhsari, T. Carmon, A. Scherer, and K. J. Vahala, Phys. Rev. Lett. **95**, 033901 (2005).
[6] C. H. Metzger and M. K. Karrai, Nature (London) **432**, 1002 (2004).
[7] F. Marquardt, J. G. E. Harris, and S. M. Girvin, Phys. Rev. Lett. **96**, 103901 (2006).
[8] M. Eichenfield, R. Kamacho, J. Chan, K. J. Vahala, and O. Painter, Nature (London) **459**, 550 (2009).
[9] D. Navarro-Urrios, J. Gomis-Bresco, S. El-Jallal, M. Oudich, A. Pitanti, N. Capuj, A. Tredicucci, F. Alzina, A. Griol, Y. Pennec, B. Djafari-Rouhani, A. Martinez, and C. M. Sotomayor Torres, AIP Adv. **4**, 124601 (2014).
[10] L. Mercadé, L. L. Martín, A. Griol, D. Navarro-Urrios, and A. Martínez, Nanophotonics **9**, 3483 (2020).
[11] I. Ghorbel, F. Swiadek, R. Zhu, D. Dolfi, G. Lehoucq, A. Martin, G. Moille, L. Morvan, R. Braive, S. Combri, and A. Rossi, APL Photonics **4**, 116103 (2019).
[12] J. Capmany and D. Novak, Nat. Photonics **1**, 319 (2007).
[13] U. Kemiktarak, M. Durand, M. Metcalfe, and J. Lawall, Phys. Rev. Lett. **113**, 030802 (2014).
[14] W. E. Lamb, Phys. Rev. **134**, A1429 (1964).
[15] G. J. Hall, M. Ebrahimzadeh, A. Robertson, G. P. A. Malcolm, and A. I. Ferguson, J. Opt. Soc. Am. **B 10**, 2168 (1993).
[16] B. E. A. Saleh and M. C. Teich, *Fundamentals of Photonics* (Wiley, New York, 1991).
[17] D. Meschede, *Optics, Light, and Lasers* (Wiley-VCH, New York, 2017).
[18] S. A. Diddams, K. Vahala, and T. Udem, Science **369**, eaay3676 (2020).
[19] C. Metzger, M. Ludwig, C. Neuenhahn, A. Ortlieb, I. Favero, K. Karrai, and F. Marquardt, Phys. Rev. Lett. **101**, 133903 (2008).
[20] J. Sheng, X. Wei, C. Yang, and H. Wu, Phys. Rev. Lett. **124**, 053604 (2020).
[21] E. Gil-Santos, M. Labousse, C. Baker, A. Goetschy, W. Hease, C. Gomez, A. Lematre, G. Leo, C. Ciuti, and I. Favero, Phys. Rev. Lett. **118**, 063605 (2017).
[22] G. Heinrich, M. Ludwig, J. Qian, B. Kubala, and F. Marquardt, Phys. Rev. Lett. **107**, 043603 (2011).
[23] M. Zhang, G. S. Wiederhecker, S. Manipatruni, A. Barnard, P. McEuen, and M. Lipson, Phys. Rev. Lett. **109**, 233906 (2012).
[24] C. A. Holmes, C. P. Meaney, and G. J. Milburn, Phys. Rev. E **85**, 066203 (2012).
[25] N. Lörch, S. E. Nigg, A. Nunnenkamp, R. P. Tiwari, and C. Bruder, Phys. Rev. Lett **118**, 243602 (2017).
[26] M. F. Colombano, G. Arregui, N. E. Capuj, A. Pitanti, J. Maire, A. Griol, B. Garrido, A. Martinez, C. M. Sotomayor-Torres, and D. Navarros-Urrios, Phys. Rev. Lett. **123**, 017402 (2019).
[27] K. Pelka, V. Peano, and A. Xuereb, Phys. Rev. Research **2**, 013201 (2020).
[28] G. Madiot, F. Correia, S. Barbay, and R. Braive, arXiv:2005.08896.
[29] M. Zhang, S. Shah, J. Cardenas, and M. Lipson, Phys. Rev. Lett. **115**, 163902 (2015).
[30] S. Walter and F. Marquardt, New J. Phys. **18**, 113029 (2016).
[31] I. Mahboob, H. Okamoto, and H. Yamaguchi, Sci. Adv. **2**, e1600236 (2016).
[32] M. J. Weaver, F. Buters, F. Luna, H. Eerkens, K. Heeck, S. de Man, and D. Bouwmeester, Nat. Commun. **8**, 824 (2017).
[33] H. Xu, A. A. Clerk, and J. G. E. Harris, Nature (London) **568**, 65 (2019).
[34] J. P. Mathew, J. del Pino, and E. Verhagen, Nat. Nanotechnol. **15**, 198 (2020).
[35] C. F. Ockeloen-Korppi, E. Damskägg, J. M. Pirkkalainen, M. Asjad, A. A. Clerk, F. Massel, M. J. Wooley, and M. A. Sillanpää, Nature (London) **556**, 478 (2018).
[36] See Supplemental Material at http://link.aps.org/supplemental/10.1103/PhysRevLett.127.073601 for a broader description of the analytical treatments as well as the deeper insight into the experimental mechanical characterization.
[37] M. Seimetz, *High-Order Modulation for Optical Fiber Transmission* (Springer, New York, 2009).
[38] D. Malz and A. Nunnenkamp, Phys. Rev. A **94**, 023803 (2016).
[39] I. Pietikäinen, O. Černotik, and R. Filip, New J. Phys. **22**, 063019 (2020).
[40] C. Genes, A. Mari, D. Vitali, and P. Tombesi, Adv. At. Mol. Opt. Phys. **57**, 33 (2009).
[41] M. Karuza, C. Molinelli, M. Galassi, C. Biancofiore, P. Natali, A. Tombesi, G. Di Giuseppe, and D. Vitali, New. J. Phys. **14**, 095015 (2012).
[42] P. E. Kloeden and E. Platen, *Numerical Solution of Stochastic Differential Equations* (Springer-Verlag, Berlin-Heidelberg, 1992).
[43] M. Oudich, S. El-Jallal, Y. Pennec, B. Djafari-Rouhani, J. Gomis-Bresco, D. Navarro-Urrios, C. M. Sotomayor Torres, A. Martínez, and A. Makhoute, Phys. Rev. B **89**, 245122 (2014).
[44] A. Pikovsky, M. Rosenblum, and J. Kurths, *Synchronization: A Universal Concept in Nonlinear Sciences* (Cambridge University Press, Cambridge, England, 2003).
[45] E. Rubiola, *Phase Noise and Frequency Stability in Oscillators* (Cambridge University Press, Cambridge, England, 2009).

[46] S. Tallur, S. Sridaran, and S. A. Bhave, Opt. Express **19**, 24522 (2011).
[47] S. Sridaran and S. A. Bhave, *Proceedings of the 2012 IEEE 25th International Conference on Micro Electro Mechanical Systems (MEMS), Paris, France* (IEEE, New York, 2012), p. 664667, https://ieeexplore.ieee.org/document/6170083.
[48] X. Luan, Y. Huang, Y. Li, J. F. McMillan, J. Zheng, S. Huang, P. Hsieh, T. Gu, D. Wang, A. Hati, D. A. Howe, G. Wen, M. Yu, G. Lo, D. Kwong, and C. W. Wong, Sci. Rep. **4**, 6842 (2014).
[49] D. W. Allan, N. Ashby, and C. C. Hodge, *The Science of Timekeeping, Application Note 1289* (Hewlett Packard, Palo Alto, 1997).
[50] W. Yu, W. C. Jiang, Q. Lin, and T. Lu, Nat. Commun. **7**, 12311 (2016).
[51] D. Antonio, D. H. Zanette, and D. López, Nat. Commun. **3**, 806 (2012).
[52] M. C. Cross, Phys. Rev. E **85**, 046214 (2012).
[53] P. Kharel, G. I. Harris, E. A. Kittlaus, W. H. Renninger, N. T. Otterstrom, J. G. E. Harris, and P. T. Rakich, Sci. Adv. **5**, eaav0582 (2019).